

Breast Cancer Diagnosis by Higher-Order Probabilistic Perceptrons

Aditya Cowsik¹ and John W. Clark^{2,3}

¹*Physics Department, Princeton University, Princeton, NJ 08540*

²*McDonnell Center for the Space Sciences & Department Physics,
Washington University, St. Louis, MO 63130, USA*

³*Centro de Investigação em Matemática e Aplicações, University of Madeira,
9020-105 Funchal, Madeira, Portugal 9000-390 Funchal, Madeira, Portugal*

A two-layer neural network model that systematically includes correlations among input variables to arbitrary order and is designed to implement Bayes inference has been adapted to classify breast cancer tumors as malignant or benign, assigning a probability for either outcome. The inputs to the network represent measured characteristics of cell nuclei imaged in Fine Needle Aspiration biopsies. The present machine-learning approach to diagnosis (known as HOPP, for higher-order probabilistic perceptron) is tested on the much-studied, open-access Breast Cancer Wisconsin (Diagnosis) Data Set of Wolberg et al. This set lists, for each tumor, measured physical parameters of the cell nuclei of each sample. The HOPP model can identify the key factors – input features and their combinations – most relevant for reliable diagnosis. HOPP networks were trained on 90% of the examples in the Wisconsin database, and tested on the remaining 10%. Referred to ensembles of 300 networks, selected randomly for cross-validation, accuracy of classification for the test sets of up to 97% was readily achieved, with standard deviation around 2%, together with average Matthews correlation coefficients reaching 0.94 indicating excellent predictive performance. Demonstrably, the HOPP is capable of matching the predictive power attained by other advanced machine-learning algorithms applied to this much-studied database, over several decades. Analysis shows that in this special problem, which is almost linearly separable, the effects of irreducible correlations among the measured features of the Wisconsin database are of relatively minor importance, as the Naive Bayes approximation can itself yield predictive accuracy approaching 95%. The advantages of the HOPP algorithm will be more clearly revealed in application to more challenging machine-learning problems.

PACS numbers: 02.50.Tt,02.60.Ed,05.65.+b,07.05.Mh,89.20.Ff,89.75.Fb

I. INTRODUCTION

We shall describe a new machine-learning technique for breast-cancer diagnosis having a basis in Bayesian probability theory that not only achieves accurate classification of fine-needle aspiration biopsies but also (i) directly yields a prediction of the probability of malignancy and (ii) provides for systematic analysis of the effects on this prediction of irreducible correlations among the measured features of cell nuclei. The motivation for such research stems from the sheer magnitude of the problem posed by breast cancer: Among the various health and medical problems confronting our society to-day breast cancer is one of the most serious. The statistical data [1] released by the American Cancer Society show that except for skin cancer, breast cancer has the highest frequency of occurrence among women, apart from skin cancer. About 12% of women in the US alone will develop invasive breast cancer at some time in their lives, and during the year 2019 it is estimated that 268,000 women will have received this diagnosis. There are more than 3 million breast cancer survivors in the US who have to be monitored regularly for recurrence [1].

Even though regular screening through physical examination and mammograms of most women above the age of 35 \sim 40 is being conducted, a definitive diagnosis of any discovered lesion or tumor requires cytological study of the cells extracted from the tumor. Fine Needle Aspi-

ration Biopsy (FNAB) is the least invasive procedure in support of such a diagnosis [2]: A very fine needle is inserted into the cyst or tumor to remove a small sample of fluid, cells, and tissue, which is then transferred to a slide and prepared for examination under a microscope. A set of such slides is examined carefully by an expert pathologist, noting various features such as agglomerations of cells and distortions in the shapes and sizes of cell nuclei as a basis for diagnosis. Digital photography and computer-aided image processing facilitate this process. The magnitude of the challenge faced by the medical profession in diagnostics and treatment is scaled not only by the prevalence of the disease and the difficulties of treatment, but also by the enormous number of biopsies that must be performed and evaluated.

One of the earliest successes in meeting the latter challenge with emerging classification technologies is that of Wolberg et al. [3–8, 13], who applied digital image analysis together with a variant of the MSM-Tree multi-surface method [9–12] to achieve automatic classification of tumors as benign or as malignant on the basis of FNAB biopsies. This pioneering step has been followed by a prodigious flow of research in the same spirit, involving the development and application of artificial neural networks and other automated learning systems to breast-cancer diagnosis [14–82]. Computer-assisted diagnosis of breast cancer has been reviewed in Ref. [83]. Computational studies comparing the performance of diverse clas-

sifier algorithms applied this problem may be found in Refs. [84–90], as well as many of the targeted studies already cited. For incisive commentary on the role of machine learning in medical diagnosis, see Ref. [92]; for warnings about misuses of neural networks classifiers for cancer diagnosis, see Ref. [93]. A survey of expert systems in their broader applications has been provided in Ref. [94], and more specifically to medical diagnosis, in Ref. [95].

The work reported here was undertaken in this context. Numerous computational strategies implemented previously in the research cited above have achieved a high level of accuracy in the diagnosis of breast cancer based on Fine-Needle Aspiration Biopsies (FNAB). While these methods are able to efficiently classify such biopsies as benign or malignant, there has been less attention has been given in determining, among the 10 to 30 characteristics or features of cell nuclei measured in creating the Wisconsin database, those specific features – *especially in combination* – that are most crucial for correct diagnosis. Knowledge of such incisive determinants could potentially yield new insights into the underlying biophysical and biochemical factors responsible for malignancy. As will be seen, the extent to which this is practical depends largely on the intrinsic difficulty of the classification problem in question.

II. HIGHER-ORDER PROBABILISTIC PERCEPTRON

Over the past four decades many pattern-classification techniques and algorithms have been developed by applied mathematicians, engineers, and physicists [96–101]. Those based on “artificial intelligence” as represented by feedforward neural network systems [97], Bayesian network models [98], and support vector machines [99] are the most relevant to the present work. Having a set of input patterns whose classifications are known *a priori*, such systems can be trained to classify new input patterns having previously unknown class assignments. We intend not only to classify biopsies into two sub-classes: (a) benign and (b) malignant, but also to predict the probability that any sample is malignant. Moreover, we will explore the prospects for identifying the specific factors derived from FNAB that are most instrumental to such classification.

The unique properties of the higher-order probabilistic HOPP model developed by Clark et al. [102] are especially suited to the task of identifying such crucial factors in a rather general category of classification problems. Figs. 1 and 2 compare two familiar architectures for feedforward neural networks. In contrast to the rather opaque multilayer neural networks in extensive use, the HOPP model has the transparent architecture of the elementary two-layer perceptron [103], without any hidden intermediate layers [102, 104]. The compensating complication relative to conventional neural-network classifiers

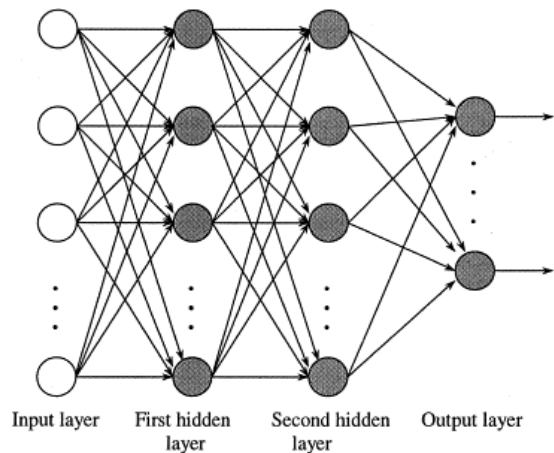


FIG. 1: Conventional multilayer feedforward neural network having two intermediate layers of “hidden neurons” between input and output layers. Darkened circles represent processing units analogous to neurons; lines oriented forward symbolize weighted connections between units analogous to interneuron synapses. Information flows left to right as units in each layer simulate those in the next layer. Such networks are commonly taught to recognize and classify input patterns via the backpropagation algorithm [100].

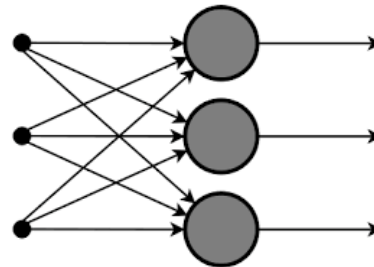


FIG. 2: Two-layer feed-forward architecture of the Rosenblatt’s Elementary Perceptron [103] and the Higher-order Probabilistic Perceptron (HOPP) [102]. Meaning of circles and lines is the same as in Fig. 1.

is that the HOPP model must allow for the inclusion of all higher-order couplings of all subsets of input units to each output unit, not just the simple neuron-neuron couplings involving a single input neuron and a given output neuron (along with single-neuron biases/thresholds), which govern the dynamics of standard neural-network models. Clark et al. have demonstrated that the HOPP architecture is sufficiently general for the full array statistical correlations among measured variables that is inherent to Bayesian inference for such a problem are incorporated. This means that the effects of correlations between the input variables on output decisions can, in practice, be made explicit through systematic determination of the higher-order couplings by training the HOPP network on a sufficiently representative database.

The Elementary Perceptron is the “primitive” of feed-forward neural-network architectures. Generalization to the Multilayer Perceptron structure adds a dimension of

depth, allowing for the representation of the data as a hierarchy of feature maps that are implemented in successive layers. The more layers, the deeper the network, hence the current focus on *Deep Neural Networks*. In the same spirit, one may add “width” to the Elementary Perceptron by enriching its single processing layer with higher-order couplings of its neuron-like units, corresponding to the introduction, in the physics of many-body systems, of three-body, four-body, \dots , K -body interactions along with familiar two-body interactions provided, for example, by the Coulomb potential.

Naturally, one may also add *width* in different way to Multilayer Perceptrons by increasing the numbers of hidden neurons in intermediate layers. Moreover, an even more general architecture may be created by allowing for higher-order couplings of the model neurons in Deep Neural Networks.

III. HOPP MODEL WITH CONTINUOUS INPUTS

In order to classify of the breast tumors of the Wisconsin Breast Cancer Database (WBCD), we have trivially adapted the HOPP model to accept continuous inputs, in such a way as to exclude self-correlations of arbitrary order. The absence of hidden intermediate layers between the input and the output layers allows us to explicitly access both the direct effects of specific inputs and the effects of all correlations among them, in principle to all relevant orders, after completion of the training process. One may well be concerned that with inputs corresponding to 10 to 30 characteristics, the total number of coupling coefficients (“weights”) in the network will become too large with increasing correlation order for this approach to be useful, because this tends to cause overfitting at the expense of generalization. However, the HOPP model admits effective pruning procedures [102]) that can operate during the training process to limit the final set of couplings to a few 10’s in the present case, while still achieving reliable classification of new cases. In the general context of medical diagnosis, success in identifying a reduced set of weights as the most salient salient might provide valuable clues to the nature of the underlying mechanisms, potentially at the molecular level, of the illness or malfunction in question.

A continuous-input version of the HOPP model suitable for classification of breast tumors features an input layer of K units having real-value activities x_1, x_2, \dots, x_K , one such unit for each of the measured features of the cell nuclei of the biopsy. Each of $L = 2$ output units λ , which respectively signal malignant and benign conditions, receives stimuli from all possible *combinations* of input units, in the form of a product of the activities of the inputs involved, weighted by a real-number factor specific to each combination. Explicitly, the un-normalized output of processing unit λ is given

by

$$u_\lambda(\mathbf{x}) = w_{\lambda,0} + \sum_{i=1}^K w_{\lambda,i} x_i + \sum_{i<j} w_{\lambda,ij} x_i x_j + \sum_{i<j<k} w_{\lambda,ijk} x_i x_j x_k + \dots + \sum_{i_1<i_2<\dots<i_K} w_{\lambda,i_1 i_2 \dots i_K} x_{i_1} x_{i_2} \dots x_{i_K}, \quad (1)$$

which includes a bias parameter $w_{0,\lambda}$ assigned to output λ .

This expression can be evaluated for any input vector $\mathbf{x} = (x_1, x_2, \dots, x_K)$. The “order” n assigned to a given term in the expansion is the equal to the number of inputs $x_{i_1}, x_{i_2}, \dots, x_{i_n}$ involved, also indicated by the labeling of weight factors $w_{\lambda,i_1,i_2,\dots,i_n}$ that appear. (For example $w_{\lambda,4,8,7}$ implies third order.) In zeroth order, there just the single bias parameter $w_{0,\lambda}$. Stopping at the second term, of order $n = 1$, one has what is known as the Naive Bayes classifier, corresponding to the assumption of *independent* input variables – hence uncorrelated. The successive terms $n = 2, 3, \dots, K$ introduce correlations among two inputs, three inputs, etc., up to all K inputs. The n th sum in the expansion (1) contains $K!/(K-n)!n!$ terms. In practice, this expansion is truncated at some maximum order $n_{\max} \equiv N$. As a technical matter, it will be convenient to regard the bias parameter $w_{\lambda,0}$ as the weight of a connection to unit λ from a fictitious input 0 with constant activity $x_0 = 1$.

We emphasize that the restrictions imposed on the sums over input indices i, j, k, \dots ensure the absence of contributions from “self-coupling” weights (or “self-correlations”) that refer to identical inputs, such as $w_{\lambda,ii} x_i^2$. Accordingly, the sums run over *irreducible* correlations among the input variables. In this respect, the HOPP model differs from the most general polynomial neural network, while providing a clean separation of correlation orders as defined above.

For any given set of weights, the raw output $u_\lambda(\mathbf{x})$ is converted to a normalized probability distribution by processing it through the following sigmoid “squashing function”:

$$y_\lambda(\mathbf{x}) = \frac{e^{u_\lambda(\mathbf{x})}}{\sum_{i=1}^L e^{u_i(\mathbf{x})}}. \quad (2)$$

This function has several useful properties, as shown by Clark et al. [102] for binary inputs and a finite number of outputs L . As already indicated, the architecture of the HOPP model is sufficiently general to embody the full statistical correlations inherent in the Bayesian approach. A full derivation of this property in the case of binary inputs may be found in Ref. [102]; an abbreviated version is provided in the Appendix. Under the restriction to binary inputs, the model simply recapitulates both the structure and content of of Bayes Rule, with $y(\mathbf{x})$ being rigorously identified with the Bayesian-optimal *a posteriori* probability in the limiting sense defined. Even though

the proof given does not apply for continuous inputs, the structure of the HOPP network is surely general enough to represent with arbitrary precision any input-output function of practical interest, although one must expect the interpretation of its output as the ideal Bayesian *a posteriori* probability to be degraded by the deviation from binary input coding.

IV. TRAINING ALGORITHM & MODEL DEVELOPMENT

In order to achieve optimal classification, the weights \mathbf{w} must be adjusted via a training process. The objective is to minimize the difference between the probability estimates y_λ and the actual binary values a_λ known independently for each of a given set of input vectors \mathbf{x} . This difference is interpreted in the mean-square sense, so the cost function to be minimized is

$$E = \sum_{\lambda} (y_\lambda - a_\lambda)^2. \quad (3)$$

In this paper we adopt a gradient-descent method to arrive at the best set of weights for the given data set. Two parameters $\epsilon > 0$ (the learning rate) and $\mu < 0$ (called the momentum) and serve to control the speed and smoothness of descent [100]. Specifically, the incremental learning rule is taken as

$$\Delta w(t) = \epsilon(a_\lambda - y_\lambda) \frac{\partial u_\lambda}{\partial w} + \mu \Delta w(t-1). \quad (4)$$

In this familiar expression, $\Delta w(t)$ is the weight correction made in the time step from $t-1$ to t , with w as shorthand for the complete set of nonzero weights, which have the generic form $w_{\lambda, k_1 k_2 k_3 \dots x_{k_1} x_{k_2} x_{k_3} \dots}$.

We now describe the steps involved in the implementations of the routine implied by Eq. (4) and developing HOPP models capable of reliable generalization.

It is apparent from Eq. (1) that the number W of connection weights increases super-exponentially as the order n increases: one is faced with a potential combinatorial explosion. To examine this feature more quantitatively, let us focus on the case $L = 2$ and $K = 30$ that applies for the problem of breast-cancer diagnosis when all input features X_i are imposed on the network. First we note the trivial fact that the probabilistic constraint $y_1 + y_2 = 1$ on the output signals y_λ reduces the number of independent weight parameters by half leaving only one free parameter in zeroth order ($n = 0$). By virtue of this constraint, one of the two output units becomes redundant, as it must necessarily produce the complement of the output of its partner. Therefore only a *single* output unit λ is needed in the two-class problem. In the present application it could indicate the probability of malignancy. Similarly, for the general classification problem involving L classes, the HOPP network requires only $L - 1$ outputs.

Thus, to zeroth order in the expansion in irreducible correlations among the inputs, there is only the single bias parameter $w_{\lambda,0}$. With first-order terms present in Eq. (1), we recover the Naive Bayes classifier. An additional $K = 30$ parameters are introduced, corresponding to the connection weights appearing in the second term of expression (1) for u_λ . Already at $n = 2$ (leading order in *correlations* among *inputs*), the total number of adjustable parameters has climbed to $465 + 1 = 466$, increasing to 4526 at $n_{\max} \equiv N = 3$, and by $N = 4$, the count has come to 31,931. Due to the prospect or inevitability of overfitting, it becomes imperative to curtail such rapid growth of degrees of freedom. (For $K = 10$, also considered in our modeling explorations, the situation is less serious, with corresponding parameter counts 11, 56, 176, and 386 at $N = 1, 2, 3$, and 4, respectively.)

To deal with this computational complexity, we have adopted the following strategy, which has proven both practical and effective.

- Given the database for the problem, consisting of a set of input vectors \mathbf{x} with known class assignments, one selects a subset – the training set T – to be used in training the network model.
- In initializing the network, all weights are set to zero, *except that* 500 weights belonging to orders 0 to $n_{\max} = N$ are given non-zero values drawn randomly from a uniform distribution on the interval $[-1.5, 1.5]$.
- Presenting each of the P_T vectors of this training set in turn, each surviving weight is processed through the learning rule (4), as the time parameter t is advanced in unit steps.
- Next, the vectors of the training set are permuted randomly among themselves, and the process of training continues as before. After repeated training cycles for 500 such randomized permutation sets, the set of fully evolved weights is culled to yield a chosen maximum of W surviving weights, priority being given to those of largest absolute magnitude. (Note: W should be interpreted as the maximum number of weights in those special cases where the total number of adjustable weights is less than W , e.g., for the choice $W = 10$.)
- The resulting network model, is then *retrained* for 500 permutations of the set of training vectors. The number of post-culling weights are usually taken to range from $W = 10$ to 50, with 30 as a typical choice.

For breast-cancer diagnosis employing the WBCD [13] these numbers of “fitting” parameters are small enough compared with the size of the training set that overfitting can normally be avoided. In a real-world scenario subserving clinical implementation, the training can be an ongoing process, continuing for an indefinite number

of generations with new data being added to the training pool as they become available.

To provide for validation of the model, the data was arbitrarily divided into (i) a training set used to generate the model, consisting of 90% of the FNAB samples and (ii) a test set comprised of the remainder, which is not involved in the determination of weight parameters and hence the diagnostic model. Performance of the model in generalization is judged most intently in terms of the percentage of correct classifications for the test set and a measure called the Matthews correlation coefficient that removes bias due to imbalance in the frequencies of benign and malignant examples in the training set.

To assess the influence of fluctuations depending on which data were included in the training set, the whole procedure described above was repeated 300 times with different subdivisions of the database into training and test sets, thus in the end generating 300 sample network models in each of the computational experiments **P1-P6** described below. Averages were taken over the performance measures computed for each ensemble of sample networks as a basis for overall assessment of the quality of the corresponding HOPP classifier. Standard deviations from these means were also evaluated, thereby achieving an elaborate *cross-validation* of the HOPP machine-learning approach in its several versions explored here.

Several conventional measures are used to evaluate the performance of the HOPP models being developed on both training and test sets. These are specified in terms of the numbers of true-positive, false-positive, true-negative, and false-negative responses of the network for the given data set (or subset), denoted respectively by p_t , p_f , n_t , and n_f .

- *Efficiency* or *Accuracy*, defined as the ratio of correct classifications to the total number of input patterns P in the data set presented, thus $ACC = (p_t + n_t)/P$.
- *Sensitivity* $SENS = p_t/(p_t + n_f)$.
- *Specificity*, $SPEC = n_t/(n_t + p_f)$.
- *Positive Predictive Value* $PPV = p_t/(p_t + p_f)$
- *Matthews correlation coefficient*,

In addition, there is the *Matthews Correlation Coefficient*

$$MCC = \frac{p_t n_t + p_f n_f}{\sqrt{(p_t + p_f)(p_t + n_f)(n_t + p_f)(n_t + n_f)}}, \quad (5)$$

which compensates for over-representation of one of the outcomes in the given database.

The outputs of the HOPP network, y_λ , are actually probabilities lying in the continuous interval $[0, 1]$. Hence some criterion must be imposed to determine the four integers p_t , p_f , n_t , n_f entering the above performance measures. The obvious choice is to set y_λ is set equal to 0 if its actual value is less than 0.5 and to 1 otherwise. (We note that in clinical practice this criterion could be modified to reduce the number of false negatives.)

V. DATA SET

The data set used in this study is available in the public domain, compiled by Wolberg, Street, and Mangasarian [6, 13] from the investigations conducted on breast tumors at the University of Wisconsin Hospitals, Madison. In the process of Fine Needle Aspiration (FNA), a very fine hypodermic needle is inserted into the tumor and a small sample of fluid containing tissue and cells is aspirated, mounted on a slide and stained to display the nuclei in the cells. The pixelated digital images of the cells and their nuclei are then subjected to a semi-automatic measurement procedure, aided by a computer. In the image of a given sample, the nuclei are separated from the rest of the image, and an approximate boundary is determined for each nucleus. This boundary is treated as a list of points, each centered on a pixel. For the definitions given below, the boundary will be represented by the list of vectors \mathbf{b}_p that correspond with the points specifying the nuclear boundary, such that the last point, \mathbf{b}_N , and the first point, \mathbf{b}_1 , coincide (hence there are $N - 1$ distinct points). Measurements are made on each of a sample of nuclei from a given biopsy, so as to obtain values of ten geometrical features X_i , as specified below. To implement machine learning, or other approaches to diagnosis, such a biopsy is represented, in the general case [8], by the mean values \bar{X}_i obtained for the variables X_i , $i = 1, 2, \dots, 10$, together with the corresponding standard deviations $\sigma_i = [(X_i - \bar{X}_i)^2]^{1/2}$ from these means and the maximum values $(X_i)_{\max}$ obtained for each geometric feature. In addition to the values of these input variables, the full Wisconsin Breast Cancer data set naturally includes the clinically validated classification of the corresponding tumor as either benign or malignant.

The ten measured characteristics or features of cell nuclei underpinning the Wisconsin Breast Cancer Database (WBCD) are:

- **Radius** X_1 . The center of the nucleus, \mathbf{c} , is defined to be the average of the points on the boundary. The radius of the nucleus is defined as the average distance between the points on the boundary and the center point, i.e.

$$X_1 = \frac{\sum_{i=1}^{N-1} \|\mathbf{b}_i - \mathbf{c}\|}{N - 1}. \quad (6)$$

- **Texture** X_2 The texture of the nucleus is the variance of gray-scale intensities in the component pixels inside its boundary.
- **Perimeter** X_3 . The perimeter of the nucleus is defined as the sum of the distances between points as follows:

$$X_3 = \sum_{i=1}^{N-1} \|\mathbf{b}_{i+1} - \mathbf{b}_i\|. \quad (7)$$

- **Area** X_4 . This is defined as the number of pixels inside the boundary of the nucleus, plus half the number of pixels on the boundary.
- **Compactness** X_5 . Observing that the circle has the maximum area for a specified value of the perimeter, the compactness is defined as the ratio of the square of the perimeter to the area.

$$X_5 = \frac{(X_3)^2}{X_4}. \quad (8)$$

Note that “compactness” thus defined actually increases for a more diffuse nucleus.

- **Smoothness** X_6 . This feature is given by the mean absolute deviation of the length $r_i = \|\mathbf{b}_i - \mathbf{c}\|$ of a radial line with respect to the radial length of the next adjacent neighbor r_{i+1} along the perimeter. Thus

$$X_6 = \sum_{i=1}^{N-1} \frac{|r_i - (r_i + r_{i+1})/2|}{X_3}. \quad (9)$$

It is important to recognize that, as defined, X_6 *increases* as the perimeter becomes more jagged. Hence it decreases as the perimeter becomes more smooth, and so it might better be called Roughness.

- **Concavity** X_7 . This feature represents the severity of indentations on the periphery of the nucleus. To quantify it, a simple algorithm is used to construct chords between points on the perimeter so as to bound such indentations and measure the total area of the concavities so enclosed. Since the chord lengths involved are small, this feature quantifies small-scale rather than large-scale irregularities [4–6].
- **Concave Points** X_8 . This feature is similar to concavity in that it measures the number of representative points on the perimeter that lie within the concave regions of the image. In contrast to the X_7 , the magnitudes of the deviations from regularity affect this measure. It is to be noted that the measures X_7 and X_8 quantifying concavity and concave points are affected by pixelation.
- **Symmetry** X_9 . This feature actually represents the *deviations* from symmetry in the direction transverse to the major axis (defined as the longest chord passing through the center). Lines perpendicular to the major axis are drawn at regular intervals and the lengths of the intercepts, l_{ai} and l_{bi} are used to define

$$X_9 = \frac{\sum_i |l_{ai} - l_{bi}|}{\sum_i |l_{ai} + l_{bi}|}. \quad (10)$$

- **Fractal Dimension** X_{10} . Conceptually, this measure has been introduced by Mandelbrot [105], in

particular to describe an irregular boundary of two-dimensional area, such as the coastline of Norway. According to Mandelbrot’s prescription, the fractal dimension of the boundary of a cell nucleus is estimated by measuring the perimeter of its nucleus with increasingly larger “rulers.” The log of the perimeter measurements so obtained is plotted against the logarithm of the ruler size. In the limit, the magnitude of the slope of the plot gives the fractal dimension X_{10} of the nuclear perimeter [3].

Figs. 3-7 show histograms of the data extracted for the ten nuclear features X_1 through X_{10} as extracted from measurements performed on the FNA biopsies of all 569 patients. These represent approximate probability density distributions of the geometrical properties that have been singled out. Note the broad distributions and the absence of multiple peaks. A single sample would clearly present a challenge for manual diagnosis.

The fact that these figures show the distributions for all biopsies, both well and ill, suggests that one might also consider separately the distributions for benign and malignant cases, and the degrees of overlap for each feature. This could offer another route to diagnosis, which might even be extended beyond the binary benign-malignant decision to a measure of the degree of illness.

VI. STRATEGIES EXPLORED & MODEL PERFORMANCE EVALUATED

The results reported here are based on several distinct training strategies for the construction of HOPP classifiers, each with its own objective. The quality of the resulting network models is evaluated in terms of the performance measures listed in Section 5, namely: accuracy ACC (or efficiency), sensitivity SENS, specificity SPEC, positive predictive power PPV (or precision), and the Matthews correlation coefficient MCC defined by Eq. (5). Since we are primarily concerned with performance in prediction or “generalization,” we focus on the measures ACC and MC obtained for the test sets, but some results are also also quoted for the other three measures. Of course, one is also interested the quality of the model in reproducing known cases, i.e., “quality of fit,” which is reflected in the results for the five performance measures on the training sets.

It is well to note here that the above performance measures refer to strict yes-or-no decisions, whereas the HOPP network model automatically yields a *probability estimate* for malignancy and its complementary estimate for a benign condition. This actually presents no problem, in that the lack of ambiguity is ensured by the strongly bivalent character of the network output, as clearly documented in our results.

We present here a summary what has been learned from a large number of computer experiments carried out

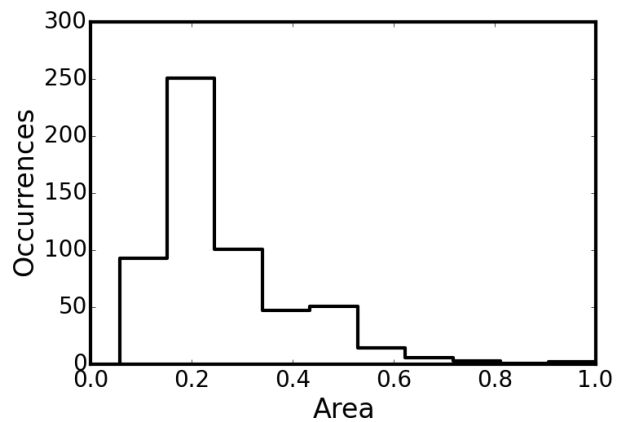
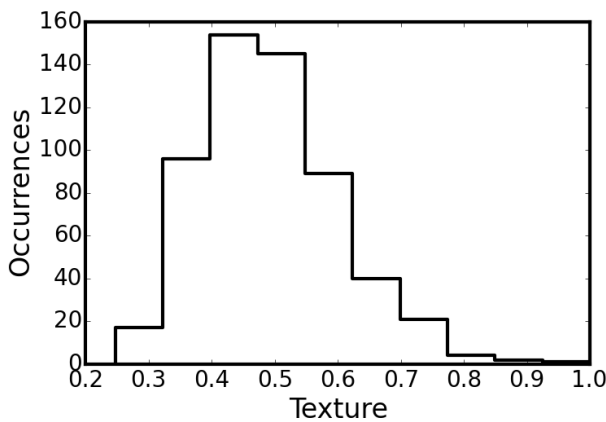
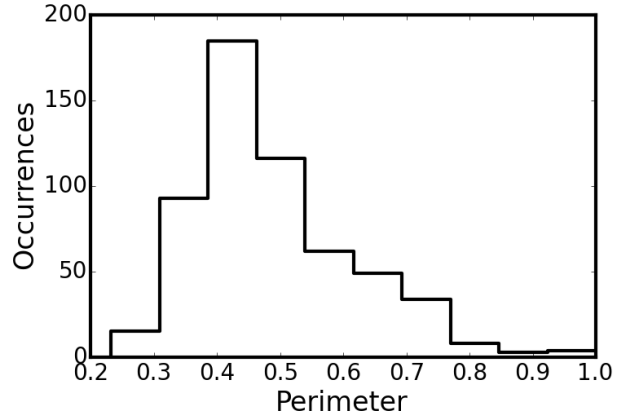
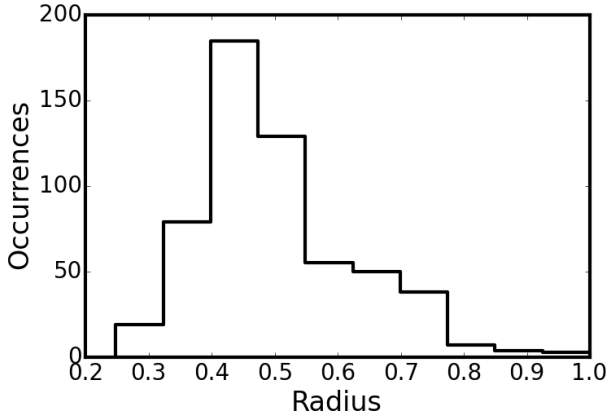


FIG. 3: Frequencies of occurrence (approximate probability densities) of different values of input features X_1 (left panel) and X_2 (right panel), normalized as specified in the text and plotted as normalized distributions among bins of each measured variable. These features correspond respectively to the sample means of radius and texture metrics as determined in FNA biopsies of the 569 patients of the Wisconsin data set.

according to eight alternative training protocols. The reader has access to a set of tables providing detailed results for all eight protocols at <http://physics.wustl.edu/people/john-w-clark>.

- **Procedure 1 (P1)** In our initial approach to model development, all of the $K = 30$ features X_1, \dots, X_{30} determined for the FNA biopsies were used in constructing the neural-network classifiers. Weights of order $n = 3$ or lower were included among those sampled, i.e., $N = 3$, so weights as complicated as $w_{\lambda,ijk}$ are included.

- The HOPP networks constructed are able to classify 95.70% of the 300 *test sets* correctly *on average*, i.e., with an average accuracy $\text{ACC} = 0.9570$ on the model ensemble, with standard deviation 0.0273.

FIG. 4: As in Fig. 2 but for input features X_3 and X_4 corresponding respectively to sample means of perimeter and area metrics.

The corresponding result for the Matthews coefficient MCC is 0.9077 ± 0.0589 , and for the other performance measures we find $\text{SENS} = 0.9767 \pm 0.0256$, $\text{SPEC} = 0.9234 \pm 0.617$ and $\text{PPV} = 0.9559 \pm 0.0351$. The quality measures achieved on the *training sets* in this computer experiment are $\text{ACC} = 0.9703 \pm 0.0053$ and $\text{MCC} = 0.9364 \pm 0.0114$, $\text{SENS} = 0.9836 \pm 0.0052$, $\text{SPEC} = 0.9480 \pm 0.0083$, and $\text{PPV} = 0.9696 \pm 0.0048$. Such performance was realized with $W = 30$ post-culling weights (plus the two biases). Such performance was realized with $W = 30$ post-culling weights (plus the two biases). It is likely that a slight improvement $\sim 1-2\%$ can be gained by adjusting this choice. Some of the sample models among the 300 involved in cross-validation process demonstrated perfect classification.

- As described in Section 4, a thorough cross-validation process was implemented by the creation

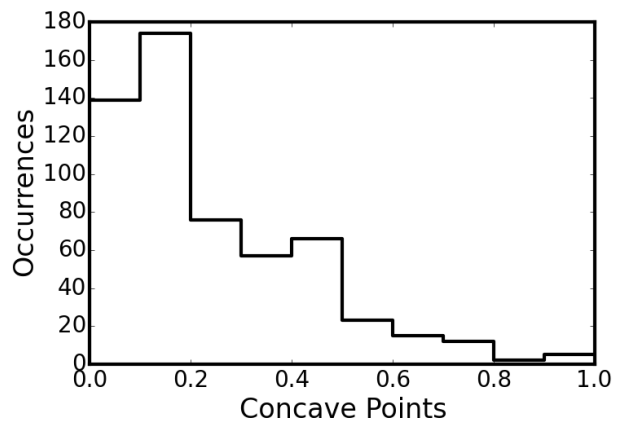
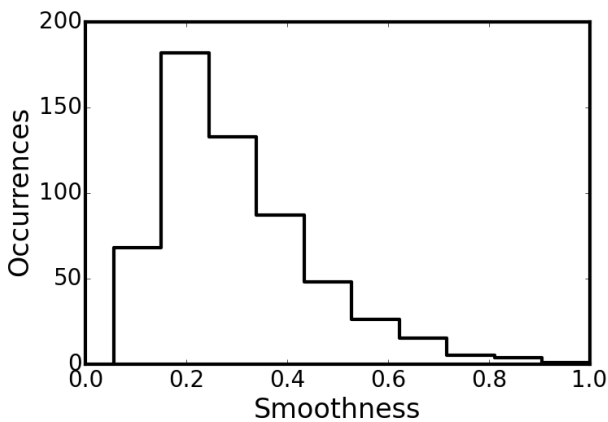
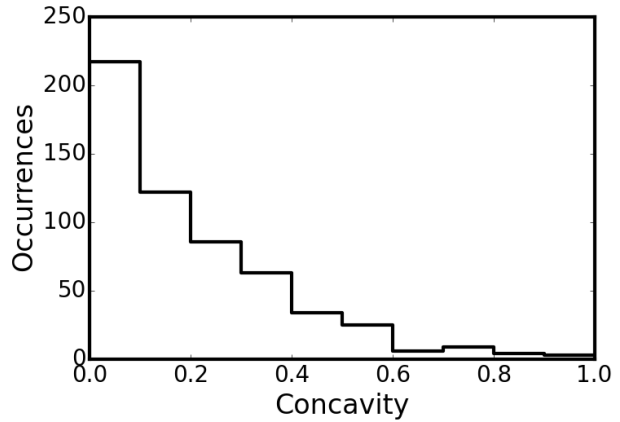
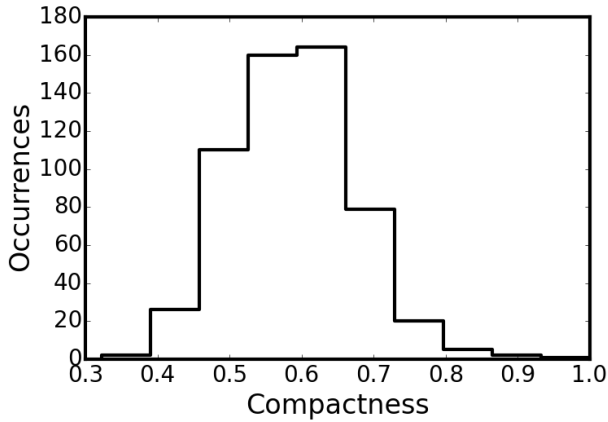


FIG. 5: As in Fig. 2 but for input features X_5 and X_6 corresponding respectively to sample means of compactness and smoothness metrics.

FIG. 6: As in Fig. 2 but for input features X_7 and X_8 corresponding respectively to sample means of concavity and concave points metrics.

of 300 HOPP models for 300 different randomly generated subdivisions of the database into training and test sets. The results summarized in (i) provide an unambiguous demonstration of the reliability of the HOPP classifier, with additional evidence to be provided in further numerical experiments. For all five performance measures, the standard deviations from the corresponding means are very small, at most a few percent of the means.

- **Procedure 2 (P2).** To provide a baseline case that has been studied in previous machine-learning studies of this classification problem, we revert to the Naive Bayes classifier, thus stopping at first order in irreducible correlations, ignoring the higher-order interactions in Eq. (1). Thus we truncate the expansion at $N = 1$, thereby allowing for weights of the form $w_{\lambda,i}$ (along with the biases b_λ). In a first modeling exercise, the number weights was culled to a maximum W of 30. In this case, the 300 net-

work models that were created during cross validation attained an ensemble-average ACC of 0.966 and mean Matthews coefficient MCC of 0.928 on the test sets, hence even slightly better predictive performance than that found to third order by procedure **P1**, also for 30 surviving non-trivial weights. With 50 remaining weights, the average performance figures on the test sets improved to ACC = 0.9725 and MCC = 0.9411, the corresponding results for the training set being 0.9866 and 0.9714, respectively. One must conclude that with all 30 available inputs, the Naive Bayes classifier by itself can already display splendid performance. The quantitative effectiveness of this simple algorithm for the Wisconsin database has been documented previously in Refs. [77, 81] (In this special classification problem, it seems that “we can put all our eggs in one basket.”)

- **Procedure 3 (P3).** In a third model-development

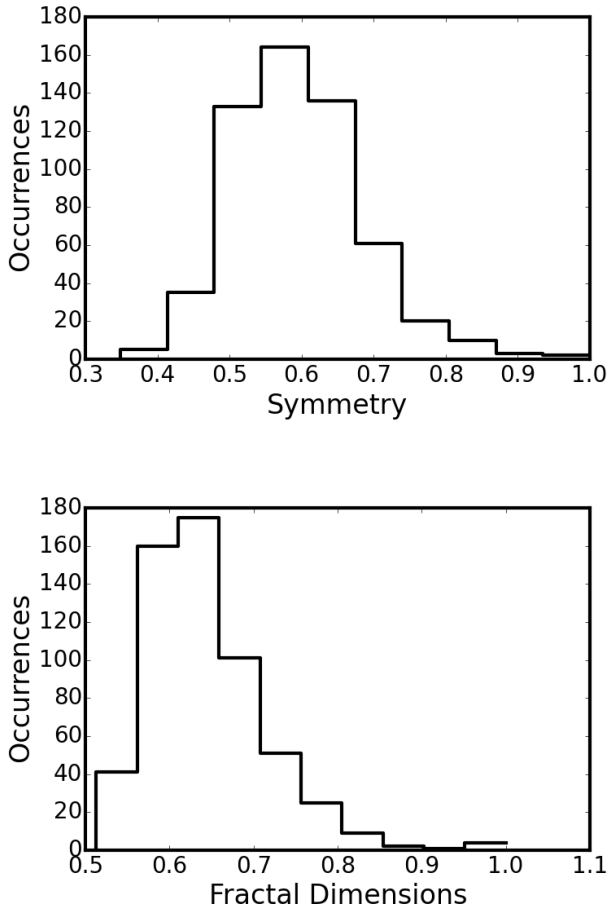


FIG. 7: As in Fig. 2 but for input features X_9 and X_{10} corresponding respectively to sample means of symmetry and fractal dimension metrics.

exercise, the set of input features used in training was restricted to the *mean values* \bar{X}_i of the ten measured quantities X_1, \dots, X_{10} . One motivation of this experiment was to test the sensitivity of predictive performance of the HOPP model to a reduction in the number of input parameters used to characterize the space in which the diagnostic problem is modeled. Again 300 network models were developed in cross-validation runs, now with the number of post-culling weights W ranging from 10 to 40 in steps of 10. Thus, four sets of cross-validation runs were made for each choice of the maximum order N retained in the correlation expansion (1), which ranged from 1 (Naive Bayes) to 4. In this case, the best test-set results at the Naive Bayes level, obtained at $W = 20$, are $\text{ACC} = 0.9373 \pm 0.0327$ and $\text{MCC} = 0.8656 \pm 0.0701$, along with $\text{SENS} = 0.9572 \pm 0.0378$, $\text{SPEC} = 0.9040 \pm 0.0647$, and $\text{PPV} = 0.9440 \pm 0.0377$. Overall, the *optimal* results on the test ensemble are found at

second order, $N = 2$, and $W = 20$: $\text{ACC} = 0.9427 \pm 0.0292$ and $\text{MCC} = 0.8770 \pm 0.0620$, with $\text{SENS} = 0.9606 \pm 0.0342$, $\text{SPEC} = 0.9121 \pm 0.0625$, and $\text{PPV} = 0.9497 \pm 0.0364$.

The choice of “best” model is somewhat ambiguous, depending on what aspect of the diagnosis is considered most important. For example, a physician may give priority to suppressing false negatives for presence of the disease and would then be most interested in the sensitivity of the diagnostic tool. Be that as it may, in identifying the optimal model among those generated in a given Procedure, we shall instead give priority to the accuracy or efficiency of prediction, ACC, followed by the Matthews correlation coefficient MCC. It will be seen, however, that the differences in the quality of the results obtained over the ranges of N and W considered are generally minimal; basically, the differences are in the noise. This applies to the documented performance on both test- and training-set ensembles.

With regard to the training phase, performance refers to the quality of fit, which generally improves with increasing N and W ; however, the gradual increases in the five quality indices remain below 3% over the ranges considered, and overfitting does not appear to be an issue. In the **P3** study, the training-set results at $N = 2$ and $W = 20$ are $\text{ACC} = 0.9497 \pm 0.0049$ and $\text{MCC} = 0.8924 \pm 0.0102$, with $\text{SENS} = 0.9839 \pm 0.0215$, $\text{SPEC} = 0.9661$, and $\text{PPV} = 0.9798 \pm 0.0231$.

Summarizing,

- (i) For the 10-input case based only on the mean values of the ten X_i , we find only a modest degradation in the measure ACC from the results found with Procedure 1.
 - (ii) Reinforcing what was learned in comparing the results of exercises **P1** and **P2** for the 30-input case, we again find that the Naive Bayes approximation yields results not significantly worse than the best results obtained at higher order (in this case $N = 2$), and with the same number of fitting parameters.
- **Procedure 3a (P3a)**. A clear message from exercises **P1-P3** is that for the diagnostic problem defined by the WBCD, higher-order irreducible correlations (i.e., terms with $n > 1$ in the expansion (1)) are in fact of minor importance. That being so, it might be advisable to give these higher-order effects less emphasis in the weight-culling process. With this in mind, we have repeated Procedure 3, but in deciding upon the weights to be kept, we used the n th-roots of the magnitudes of the n th-order weights, rather than the weights themselves, in establishing priority for survival.

The procedure so executed, otherwise identical to **P3** and labeled **P3a**, yielded the next-best results among all the computational procedures explored for HOPP models, if the maximum number of weights kept is restricted to $W = 30$. The optimal results on the test-set ensemble, occurring rather naturally at the Naive Bayes stage and for the choice $W = 30$, are $\text{ACC} = 0.9727 \pm 0.0196$ and $\text{MCC} = 0.9421 \pm 0.0418$. The improvement over results from **P1** and **P2** may be only marginally significant for ACC, but the improvement of the Matthews coefficient is quite striking. (In general, the latter improvement is also found for the other results obtained with this procedure.)

- **Procedure 3b (P3b)**. Complementary to **P3** and **P3a**, we have repeated **P3** for the ten inputs provided by the so-called “worst” values of the quantities X_1, \dots, X_{10} measured for cell nuclei in a given biopsy, as defined in Section 5. Significantly better results are obtained than were found for **P3**. In fact, the quality of the results obtained using this alternative to **P3** is the best achieved for any of the eight HOPP-based procedures applied to this classification problem, although **P3a** yields competitive results. However, in this case the optimal test-set performance was found at $W = 40$ weights: $\text{ACC} = 0.9772 \pm 0.0196$, $\text{MCC} = 0.9511 \pm 0.0420$, $\text{SENS} = 0.9839 \pm 0.0215$, $\text{SPEC} = 0.9661$, and $\text{PPV} = 0.9798 \pm 0.0231$. Significantly, the corresponding Naive Bayes results for $W = 30$, and even those for $W = 20$, are very close to these, notably $\text{ACC}_{W=30} = 0.9770 \pm 0.0176$, $\text{ACC}_{W=20} = 0.9769 \pm 0.0190$, $\text{MCC}_{W=30} = 0.9500 \pm 0.0394$, and $\text{MCC}_{W=20} = 0.9505 \pm 0.0411$. Moreover, the best results (versus W) for the higher-order cases $N > 1$ show only slight degradation, typically under 1%. Given the relatively small numbers of adjustable parameters in these networks, one normally expects the ensemble averages of the five performance measures obtained for the training ensembles to fall short of perfection on average. Nevertheless, they exhibit remarkably high quality. As a typical example, in the Naive Bayes case we find $\text{ACC}_{W=30} = 0.9825 \pm 0.0028$ and $\text{MCC}_{W=3} = 0.9625 \pm 0.0060$.

- **Procedure 4 (P4)**. It is of considerable interest to develop models for a *reduced set* of inputs that are judged, by some plausible criterion, to be especially most influential in successful classification. With fewer inputs, hence fewer adjustable parameters at given correlation order, one has the concomitant advantage of suppressing overfitting. This general theme was already fruitfully explored in the pathbreaking work of Wolberg and collaborators [5, 6]. They were able to identify small subsets of the standard 30 input features, which, as inputs for lower-dimensional multisurface classifiers [9–12], maintained accurate representations of the

training data while providing for good generalization to new cases. In particular, it was found that the best single-plane diagnostic classifier based on three features, namely mean Texture, worst (maximum) Area, and worst Smoothness, was able to classify 97.3% of the cases in the database correctly. The performance on cases *not* used in model construction was assessed by ten-fold cross-validation, with a predicted success rate of 97.0% on the “unseen” examples, as appraised through a ten-fold cross-validation. Interestingly, Street et al. [5] point out that the best feature triplets tend to contain a size feature, a shape feature, and a third feature of indifferent character with marginal relevance.

In procedure **P4** we have generated ensembles of HOPP models based on the same three input features employed by Wolberg et al. in the study cited above. Otherwise, this exercise follows essentially the same pattern as **P1-P3b**. We considered values of W ranging from 10 to 80 in steps of 10, for maximum orders N up to 3. The best results for the test-set ensembles were obtained at (i) $N = 1$ with $W = 80$, (ii) $N = 3$ with $W = 70$, and (iii) $N = 3$ with $W = 80$, yielding (i) $\text{ACC} = 0.9570 \pm 0.0263$, $\text{MCC} = 0.9091 \pm 0.0555$, (ii) $\text{ACC} = 0.9570 \pm 0.0259$, $\text{MCC} = 0.9087 \pm 0.0542$, and (iii) 0.9573 ± 0.0243 , $\text{MCC} = 0.9091 \pm 0.0516$. The associated training-set results have respectively (i) $\text{ACC} = 0.9565 \pm 0.0034$, $\text{MCC} = 0.9068 \pm 0.0072$, (ii) $\text{ACC} = 0.9606 \pm 0.0037$, $\text{MCC} = 0.9157 \pm 0.0078$, and (iii) $\text{ACC} = 0.9601 \pm 0.0036$, $\text{MCC} = 0.9146 \pm 0.0075$. We find as before that, within the statistical noise, the Naive Bayes classifier offers performance on a par with the best models including explicit effects of higher-order correlations. The other three test-set performance measures for the best Naive Bayes model ensemble are $\text{SENS} = 0.9681 \pm 0.0319$, $\text{SPEC} = 0.9399 \pm 0.0513$, and $\text{PPV} = 0.9632 \pm 0.0319$, while the corresponding training-set results are $\text{SENS} = 0.9692 \pm 0.0061$, $\text{SPEC} = 0.9350 \pm 0.0105$, and $\text{PPV} = 0.9618 \pm 0.0059$.

- **Procedure 5 (P5)**. Consider once again the 30 individually measured features of the cell nuclei of a given FNAB, proposed by Wolberg et al. [3] as potentially decisive evidence for reliable diagnosis, and alternatively a smaller set of 10 features consisting for example of the mean values or maximum values of the features X_1, \dots, X_{10} identified in Section 5. In either case the terms of expansion (1) beyond the Naive Bayes order $n = 1$ describe the irreducible effects of these features acting in unison, i.e., of *factors* composed of the original features. For 30 features, the same combinatoric analysis as presented in Section 4 shows that the 2nd-, 3rd-, and 4th-order correlations in this expansion give rise respectively to 466, 4526, and 31,931 *distinct*

factors, the respective counts being reduced to 46, 176, and 386 if only 10 features are employed. In a transparent notation, simple examples of such factors are: Area \times Smoothness ($n = 2$), Perimeter \times Concavity \times Symmetry ($n = 2$), and Radius \times Texture \times Compactness \times FractalDimension ($n = 4$). (For each example a choice is to be made among mean, worst-value, and standard deviation of the each property involved.)

In some classification problems, the effects of features acting *in combination* (i.e., nontrivial “factors”) may be stronger or weaker than the same features acting in isolation, i.e., there may be terms in Eq. (1 beyond the Naive Bayes approximation that play a special or even dominant role in determining the class of a given example. Execution of Procedures **P1-P4** has provided no evidence that this behavior is seriously in play for the classification task posed by the WBCD. However, in other classification problems, the following criterion might prove useful in assessing the degree of relevance of a given factor (or feature, as a special case) for successful generalization. Let the *number of appearances* A (or frequency) of a given factor in any of a set of model development runs (cross-validations) be defined as the number of times that particular factor survives in the culling process leading to an ensemble of HOPP networks. One may then rank order the factors according to the counts A for this ensemble, recognizing that there will be many degeneracies.

Appearance counts A were made in some of model-development runs described above. As expected, there was high degeneracy among the counts for various factors and individual features, there were many that appeared in all or nearly all of the 300 fully processed networks. among the 300. In an exercise that mirrors that reported in Refs. [5, 6], we have created an ensemble of 300 HOPP networks having mean values of Texture, Area, and Concave Points, which scored at or close to 300 in appearances. For these runs we considered the same ranges of N and W as in **P4**. The best results from this set of runs were found at $W = 10$ for $N = 2$. For this ensemble, the test-set results are $ACC = 0.9414 \pm 0.0306$, $MCC = 0.8741 \pm 0.0659$, $SENS = 0.9629 \pm 0.0334$, $SPEC = 0.9056 \pm 0.0690$, and $PPV = 0.9460 \pm 0.0398$, the associated training-set values being $ACC = 0.9409 \pm 0.0049$, $MCC = 0.8732 \pm 0.0102$, $SENS = 0.9624 \pm 0.0107$, $SPEC = 0.9045 \pm 0.0122$, and $PPV = 0.9444 \pm 0.0062$. However, the difference between these results and those for $W = 30$ and $N = 2$ are insignificant, with $ACC = 0.9413$. In fact ACC and MCC remain above 0.93 and 0.86, respectively, over full ranges N and W , and Naive Bayes performance, best at $W = 30$, is again statistically indistinguishable from that at $N = 2$ with $W = 10$.

• **Procedure 6: P6** As a final exercise in model development, we pursue the option of working with a binary representation of the inputs to the HOPP networks constructed. Each value of the 30 measured nuclear features was approximated by a B -bit input, with experiments performed for $B = 1, 2, \text{ and } 3$. For each choice of B , correlation orders N up to 4 were studied, with the maximum number of weights W ranging from 50 to 190 in steps of 10 for each N . The “best” results for the test-set ensembles achieved in this exercise (otherwise conducted as in the procedures above) were found for $B = 4, N = 2$ and $W = 120$, with $ACC = 0.9438 \pm 0.0314$, $MCC = 0.8786 \pm 0.0682$, $SENS = 0.9618 \pm 0.0320$, $SPEC = 0.9129 \pm 0.0669$, and $PPV = 0.9495 \pm 0.0375$. Marginally different results were found (i) at $B = 4, N = 2, W = 180, B = 4, W = N, W = 150$, (ii) $B = 3, N = 2, W = 180$, and (iv) $B = 3, N = 2, W = 170$. The corresponding training-set results for the “best” case are perfect; the same is true for cases (i)-(iv). It should be emphasized that many other ensembles show performance just as good, within the noise measures. Quite striking results were obtained for the special case of an ensemble of Naive Bayes networks in which the inputs are represented by single bits, with all adjustable weights eligible, marginally better than all the other cases: $ACC = 0.9453 \pm 0.0288$, $MCC = 0.8830 \pm 0.0614$, $SENS = 0.9673 \pm 0.0318$, $SPEC = 0.9085 \pm 0.0645$, and $PPV = 0.9468 \pm 0.0374$. Again, training-set performance was perfect.

This last alternative is of special significance from the methodological standpoint. With binary rather than continuous inputs, the resulting HOPP models possess both the architecture and input coding required for rigorous achievement of Bayes inference to given order N the expansion (1) in irreducible correlations among input variables. Aside from truncation of this expansion at finite order, the only departure from true optimal Bayesian performance stems from the limitations of the gradient-descent learning algorithm adopted for determination of the set of connection weights.

VII. DISCUSSION AND CONCLUSION

For given input data, the output of the HOPP neural network provides, by design, a probabilistic estimate that the tumor is malignant along with complementary probability that it is benign. It does not make a yes-no decision; rather, it yields further information to help the clinician to make a reasoned human decision. In this respect, the strongly bivalent behavior of the probability of malignancy shown in Fig. 8 is especially revealing. From this behavior and other aspects of the problem that have been uncovered in the development of HOPP models for

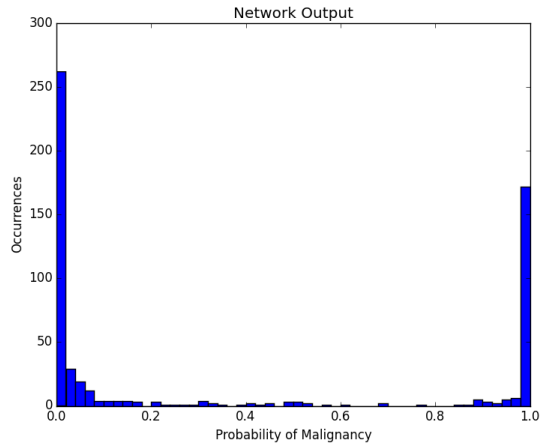


FIG. 8: Application of the network described in this paper generates an estimate of the probability of the tumor being benign or malignant. The frequency of occurrence of the different probability values for the whole data set is shown, with the resulting distribution peaking sharply at the definite benign and malignant assignments. The thin population in the middle ground may correspond to cases in which the disease is not completely expressed. The results shown were obtained for a typical network trained on all 30 measured features.

outcome prediction, the measured features of the Wisconsin Breast Cancer Database (WBCD) *overdetermine* the correct decision. Quite obviously, the redundancy among the set of features used as inputs implies that a smaller subset of them and/or their mutual correlations may well be sufficient for reliable diagnosis in clinical practice, when supplemented by the judgment of the physician. Granted this conclusion, the clear objective of future work should be to identify those minimal sets features and their combinations, which maintains maximal performance in identification of cancerous biopsies.

The results of an initial step toward this goal are summarized in Table 1 and its caption, based on the frequency with which the different factors (biopsy features and their combinations) survive the culling process in the creation of 300 candidate HOPP classifiers.

Given a database of measured physical characteristics (“features”) of the nuclei of cells extracted through Fine Needle Aspiration of breast cancer tumors, a procedure has been developed that not only provides for identification of those features most essential for correct diagnosis of a tumor, but also opens the prospect of finding those *combinations* of features that are most salient, up to arbitrary order. This program was implemented by extending the Higher-Order Probabilistic Perceptron (HOPP) model of Clark et al. [10] to continuous inputs and including, in its two-layer feedforward architecture, higher-order correlations among input variables up to fourth order. The resulting classification scheme, including 30 third-order terms, yielded a Matthews co-

efficient of 0.90 and an average predictive accuracy of 97%, with minimal deviations from this average performance from one model realization to another. These results are indicative of successful and reliable classification, with minimal sampling bias. A remarkable finding is the surprisingly high quality of performance already attained at the Naive Bayes level (first order in the expansion of the log of the predicted probability distribution). This suggests that the HOPP approach, designed to introduce effects of higher order correlations among input variables, amounts to “overkill” in this iconic machine-learning problem. The distinct advantages of the HOPP design will become more apparent in application to more challenging problems of classification and regression.

VIII. ACKNOWLEDGMENTS

This research was supported in part by the McDonnell Center for the Space Sciences. JWC is grateful for the generous hospitality of the Center for Mathematical Sciences of the University of Madeira.

IX. APPENDIX: EMBEDDING BAYES’ RULE IN A NEURAL NETWORK

An important set of problems in pattern recognition involves the classification of input patterns represented by vectors $x = (x_1, \dots, x_K)$ of finite length K . It is the task of a Classifier System to correctly assign each such input pattern to one of a finite number L of distinct categories λ (or in general to one or more categories).

It is well known [96] that Bayes’ rule provides a basis of an optimal strategy for dealing with this decision problem. One statement of Bayes’ rule (“Bayes theorem of inverse probabilities”), which follows from the definition of conditional probabilities:

The probability of an Hypothesis given the available Data is equal to the probability of the Data given the Hypothesis (“the likelihood”) times the a priori probability of the Hypothesis, divided by the a priori probability of the Data.

Applying Bayes’ rule of inference to the stated classification problem, we may assert that the posterior probability that the correct category is λ when then the input pattern is known to be x is given by

$$p(\lambda|x) = \frac{p(x|\lambda)P(\lambda)}{p(x)}, \quad (11)$$

where $p(x|\lambda)$ is the class-conditional probability that the pattern is x when the category is known to be λ (the “likelihood” of the data x) and $P(\lambda)$ is the prior probability of finding λ . (The denominator $p(x) = \sum_{\nu} p(x|\nu)P(\nu)$ is just a normalization constant ensuring

that $p(\lambda|x) \geq 0$ defines a probability distribution over exhaustive outcomes λ .)

The *Bayes-optimal decision strategy* is then to select that category μ among $\lambda = 1, \dots, L$ for which the posterior probability $p(\lambda|x)$ takes its largest value. This recipe is optimal in the sense that it minimizes the probability of misclassification.

In the simplest situation, the input variables x_1, x_2, \dots, x_K are independent of one another. This implies that the class-conditional probability $p(x|\lambda)$ must be just a product of independent factors $\rho_i(x_i|\lambda)$, one for each variable x_i . However, in principle and in practice, correlations between these variables of all orders up to K may be present in the vectors of the data ensemble. This general situation can be represented by the product decomposition

$$p(x|\lambda) = \prod_i \rho_i(x_i|\lambda) \prod_{i<j} \rho_{ij}(x_i x_j|\lambda) \prod_{i<j<k} \rho_{ijk}(x_i x_j x_k|\lambda) \cdots \rho_{1\dots K}(x_1 \dots x_K|\lambda), \quad (12)$$

where the non-negative factors ρ_{\dots} together maintain the requirement $0 \leq p(x|\lambda) \leq 1$. The $K!/m!(K-m)!$ factors $\rho_{k_1 \dots k_m}(x_{k_1} \dots x_{k_m}|\lambda)$ arising for a given order m may be different functions of their arguments.

- (i) The first product, over the $\rho_i(x_i, \lambda)$, represents the contribution to the class-conditional probability from the inputs x_i regarded as independent variables.
- (ii) The second product, over the $\rho_{ij}(x_i, x_j)$, represents the modification produced by pairwise correlations of the distinct inputs x_i and x_j .
- (iii) The third product represents the modification due to irreducible triplet correlations of the distinct inputs x_i, x_j, x_k .
- (iv) And so on to the effects of irreducible K -wise correlations.

Whether the product decomposition (or identity) is useful in practice depends on the complexity (or simplicity) of the decision tree of the classification problem. It will be useful if $p(x|\lambda)$ can be accurately approximated by the nontrivial inclusion of a relatively small number of factors in the general product, with the other factors set to their trivial values of unity. Keeping only the first \prod factor, i.e., assuming the input variables to be independent of one another, defines the *Naive Bayes Classifier* [96, 106]. Quite evidently, other representations of the posterior probability allowing for correlations among input variables are available and may prove more or less advantageous depending on the classification problem to be solved, one example being the restricted product representation adopted by Duda and Hart [96] to generate the Chow expansion. There are interesting analogies to the structure of variational wave functions employed in *ab initio* theories of quantum many-particle systems to

include effects of two-particle, three-particle, and multi-particle correlations of higher orders.

The simple steps above have exposed the essential structural requirements for a Bayes classifier in terms of an exact product decomposition of the class-conditional probability. We are now prepared to establish a precise connection with neural-network architecture. Consider a two-layer feedforward neural network consisting of: (i) K input neurons (labeled i, j, k , etc. or i_1, i_2, \dots, i_K) whose activities register the components of a given pattern vector x and (ii) L output neurons λ whose activities y_λ are to be interpreted as probabilities that the input belongs to the corresponding classes labeled $\lambda_1, \dots, \lambda_L$.

To guarantee that the outputs y_λ are positive and sum to unity, as required for a probability distribution, assume them to be given by the “soft-max” squashing function

$$y_\lambda(x) = \frac{Eq. \ e^{u_\lambda(x)}}{\sum_\nu e^{u_\nu(x)}}, \quad (13)$$

where u_λ is the net stimulus to unit λ from all the units of the input layer. The nature of the interactions between input and output neurons is still to be specified.

Thus we come to the crucial step in the constructive proof of the structural correspondence between Bayes Rule and a two-layer feedforward neural network. The Bayes posterior probability for each class λ is identified with the activity y_λ of the output neuron corresponding to that class:

$$p(\lambda|x) = \frac{p(x|\lambda)P(\lambda)}{\sum_\nu p(x|\nu)P(\nu)} = y_\lambda(x) \equiv \frac{e^{u_\lambda(x)}}{\sum_\nu e^{u_\nu(x)}} \quad (14)$$

Asserting the obvious identification

$$u_\lambda(x) = \ln[p(x|\lambda)P(\lambda)] = \ln p(x|\lambda) + \ln P(\lambda), \quad (15)$$

the quantity $\ln p(x|\lambda)$ is readily from the product representation, Eq. (12):

$$\begin{aligned} \ln p(x|\lambda) &= \sum_i \ln \rho_i(x_i|\lambda) + \sum_{i<j} \ln \rho_{ij}(x_i x_j|\lambda) \\ &+ \sum_{i<j<k} \ln \rho_{ijk}(x_i x_j x_k|\lambda) \end{aligned} \quad (16)$$

$$+ \cdots + \ln \rho_{1\dots K}(x_1 \dots x_K|\lambda). \quad (17)$$

The next task to reduce this sum-of-logs expression for the posterior probability and translate the u_λ identification into a more familiar form for the stimulus as a sum of weighted neuronal activities. To do so, we restrict considerations to the case that the input patterns are bit strings, i.e. $x_k \in \{0, 1\}$, with $k = 1, \dots, K$. Writing $1 - x_k = \bar{x}_k$ we introduce an abbreviated notation through the examples

$$\rho(x_1 = 1, x_2 = 0|\lambda) = \rho_{1\bar{2},\lambda} \quad (18)$$

and

$$\rho(x_1 = 1, x_2 = 1, x_3 = 0, x_4 = 1|\lambda) = \rho_{12\bar{3}4,\lambda}. \quad (19)$$

Next we generate a sequence of identities beginning with

$$\rho(x_1 x_2 | \lambda) = \rho_{12,\lambda}^{x_1 x_2} \rho_{1\bar{2},\lambda}^{x_1 \bar{x}_2} \rho_{\bar{1}2,\lambda}^{\bar{x}_1 x_2} \rho_{\bar{1}\bar{2},\lambda}^{\bar{x}_1 \bar{x}_2} \quad (20)$$

at the level of two correlated inputs, then to

$$\begin{aligned} \rho(x_1 x_2 x_3 | \lambda) &= \rho_{123,\lambda}^{x_1 x_2 x_3} \rho_{123,\lambda}^{x_1 x_2 \bar{x}_3} \rho_{123,\lambda}^{x_1 \bar{x}_2 x_3} \rho_{123,\lambda}^{\bar{x}_1 x_2 x_3} \rho_{123,\lambda}^{x_1 \bar{x}_2 \bar{x}_3} \\ &\times \rho_{123,\lambda}^{\bar{x}_1 x_2 \bar{x}_3} \rho_{123,\lambda}^{\bar{x}_1 \bar{x}_2 x_3} \rho_{123,\lambda}^{\bar{x}_1 \bar{x}_2 \bar{x}_3} \end{aligned} \quad (21)$$

for three, and so on for combinations of four inputs, etc., and ending with $\rho(x_1 \cdots x_K | \lambda)$.

Introducing these identities into the sum-of-logs formula (17) for the posterior probability, straightforward manipulations yield an expression for the stimulus of the output neuron λ having the form

$$\begin{aligned} u_\lambda(x) &= w_{\lambda,0} + \sum_i w_{\lambda,i} x_i + \sum_{i<j} w_{\lambda,ij} x_i x_j \\ &+ \sum_{i<j<k} w_{\lambda,ijk} x_i x_j x_k + \cdots + \\ &+ \cdots + w_{\lambda,12 \dots K} x_1 \cdots x_K. \end{aligned} \quad (22)$$

The sums are performed over *distinct* input indices 1 through K . Explicit formulas may be given for the connection weights $w_{\lambda,k_1 \dots k_m}$ and biases $w_{\lambda,0}$ in terms of the conditionals $\rho(x_{k_1} \dots x_{k_m} | \lambda)$ and the prior $P(\lambda)$, for $\lambda = 1, 2, \dots, L$. The familiar architecture of Rosenblatt’s Elementary Perceptron [103], involving only pairwise couplings from input to output neurons, is recovered upon suppression of all terms nonlinear in the input variables.

We conclude that, in general, the two-layer probabilistic network with soft-max output functions can match Bayes’ rule if and only if forward couplings from the input neurons to the output neurons of all orders up to K are permitted. Such a neural network is called a Higher-Order Probabilistic Perceptron (HOPP). Importantly, the above proof that the HOPP architecture is general enough to realize Bayes-optimal inference is based on the assumption of binary inputs, $x_i \in \{0, 1\}$. This desirable feature need not hold otherwise, and in particular for the floating-point inputs involved in the WBCD machine-learning problem.

Naturally, architecture is only part of the story, as, in effect it establishes only the class of functions that is being used to approximate the actual input-output “decision” underlying the data at hand. In real-world problems one hardly ever has direct access to the conditionals and priors needed to evaluate the weights and biases

that describe the interactions experienced by the surrogate neuronal units. In the traditional neural network context, they must be learned from examples.

As one option, it is natural to formulate a procedure for training HOPPs based on incremental gradient-descent minimization of a squared-error cost function

$$C = \frac{1}{2} \sum_\lambda^L (t_\lambda - a_\lambda)^2, \quad (23)$$

just as in backpropagation, but without the complication of hidden layers. Alternatively, a relative-entropy cost function (Kullback-Leibler entropy) may be used. It is expected that these procedures will move the weight/bias parameters ever closer to those needed to match Bayes performance, or to achieve some other optimization goal, but the sense and degree that this is being accomplished are in general elusive.

At this point, theorems established by Ruck et al. [107], Wan [108], and Richard and Lippmann [109] help clarify the situation. Two special cases are considered:

- (i) The usual case where the target (desired) outputs are “1 of L ”, meaning that one output should be unity, and all others zero.
- (ii) In the other case, the target outputs are binary, unity or zero, without regard for the number that can simultaneously take the value 1.

Inputs may be continuous or binary. To paraphrase Richard and Lippmann (1991):

- (i) When network parameters [i.e., the weights and biases] are chosen to minimize a squared-error cost function, outputs estimate the conditional expectations of the desired outputs so as to minimize the mean-squared estimation error.
- (ii) For a 1-of- L problem, when network parameters are chosen to minimize a squared-error cost function, the outputs provide direct estimates of the posterior probabilities of the Bayes classifier so as to minimize the mean-squared estimation error.
- (iii) When the desired outputs are binary but not necessarily 1-of- L and the network parameters are chosen to minimize a squared-error cost function, the outputs estimate the conditional probabilities that the desired outputs are unity, given the input.

[1] <https://www.breastcancer.org>

[2] Y.-H. Yu, W. Wei, and J.-L. Liu, Diagnostic value of fine-needle aspiration biopsy for breast mass: a systematic review and meta-analysis, BMC Cancer, 25 January

2012, 12-41.

[3] W. H. Wolberg and O. L. Mangasarian, Multisurface method of pattern separation for medical diagnosis applied to breast cancer cytologies Proc. Nat. Acad. Sci.

- USA 87 (1990) 9193-9196.
- [4] W. H. Wolberg, W. N. Street, and O. L. Mangasarian, Breast cytology diagnosis via digital image analysis, *Anal. Quant. Cytol. Histol.* 15, (1993) 396-404.
 - [5] W. N. Street, W. H. Wolberg, and O. L. Mangasarian, Nuclear feature extraction for breast tumor diagnosis, *Proc. SPIE 1905, Biomedical Image Processing and Biomedical Visualization*, 861-870 (1993).
 - [6] W. H. Wolberg, W. N. Street, and O. L. Mangasarian, Machine learning techniques to diagnose breast cancer from fine-needle aspirates, *Cancer Letters* 77 (1994) 163-171.
 - [7] O. L. Mangasarian, W. N. Street and W. H. Wolberg, Breast cancer diagnosis and prognosis via linear programming, *Operations Research* 43 (1995) 570-577.
 - [8] W. H. Wolberg, W. N. Street, and O. L. Mangasarian, Image analysis and machine learning applied to breast cancer diagnosis and prognosis, *Anal. Quant. Cytol. Histol.* 17 (1985) 77-87.
 - [9] O. L. Mangasarian, Multi-surface method of pattern separation, *IEEE Trans. on Information Theory*, IT-14 (1968) 801-807.
 - [10] O. L. Mangasarian, Mathematical programming in neural networks, *ORSA Journal on Computing* 5 (1993) 349-360.
 - [11] K. P. Bennett, Decision tree construction via linear programming, in M. Evans, ed., *Proceedings of the 14th Midwest Artificial Intelligence and Cognitive Science Society Conference* (1992), pp. 97-101.
 - [12] K. P. Bennett and O. L. Mangasarian, Robust linear programming discrimination of two linearly inseparable sets, in *Optimization Methods and Software* 1 (1992), 23-34.
 - [13] [archive.ics.uci.edu/ml/datasets/Breast+Cancer+Wisconsin+\(Original\)](https://archive.ics.uci.edu/ml/datasets/Breast+Cancer+Wisconsin+(Original)), UCI Machine Learning Repository, Irvine, CA: University of California, School of Information and Computer Science [<https://archive.ics.uci.edu/ml>].
 - [14] A. E. Dawson, R. E. Austin, D. S. Weinberg, Nuclear grading of breast carcinoma by image analysis. *Am. J. Clin. Pathol.* 95 (1991) S29-37).
 - [15] P. S. Maclin, J. Dempsey, J. Brooks, and J. Rand, Using neural networks to diagnose cancer. *J. Med. Syst.* 15 (1991) 11-19.
 - [16] P. S. Maclin and J. Dempsey, Using an artificial neural network to diagnose hepatic masses, *J. Med. Syst.* 16 (1992) 215-225.
 - [17] V. Golberg, A. Manduca, D. L. Ewert, J. J. Gisvold, J. F. Greenleaf, Improvement in specificity of ultrasonography for diagnosis of breast tumors by means of artificial intelligence, *Med. Phys.* 19 (1992) 1475-1481.
 - [18] M. L. Astion, P. Wilding, Application of neural networks to the interpretation of laboratory data in cancer diagnosis, *Clin. Chem.* 38 (1992) 34-38.
 - [19] P. Wilding, M. A. Morgan, A. E. Grygotis, M. A. Shoffner, E. F. Rosato, Application of backpropagation neural networks to diagnosis of breast and ovarian cancer, *Cancer Letters* 77 (1994) 145-153.
 - [20] P. M. Ravdin, G. M. Clark, S. G. Hilsenbeck, M. A. Owens, M.A., P. Vendely, M. R. Pandian, and W. L. McGuire, W.L., A demonstration that breast cancer recurrence can be predicted by neural network analysis, *Breast Cancer Res. Treat.* 21 (1992) 47-53.
 - [21] P. M. Ravdin and G. M. Clark, A practical application of neural network analysis for predicting outcome of individual breast cancer patients, *Breast Cancer Res. Treat.* 22 (1992) 285-293.
 - [22] W. L. McGuire, A. K. Tandon, D. C. Allred, G. C. Chamness, P. M. Ravdin, and G. M. Clark, Treatment decisions in axillary node-negative breast cancer patients, *J. Natl. Cancer Inst. Monogr. II* (1992) 173-180.
 - [23] R. Nafe and H. Choritz (1992) Introduction of a neuronal network as a tool for diagnostic analysis and classification based on experimental pathologic data, *Exp. Toxicol. Pathol.* 44 (1992) 17-24.
 - [24] Y. Wu, M. L. Giger, K. Doi, C. J. Vyborny, R. A. Schmidt, and C. E. Metz, Artificial neural networks in mammography: Application to decision making in the diagnosis of breast cancer, *Radiology* 187 (1993) 81-87.
 - [25] S. K. Rogers, D. W. Ruck, and M. Kabrisky, Artificial neural networks for early detection and diagnosis of cancer, *Cancer Letters* 77 (1994) 79-83.
 - [26] C. E. Floyd, J. Y. Lo, A. J. Yun, D. C. Sullivan, and P. J. Kornguth, Prediction of breast cancer malignancy using an artificial neural network, *Cancer* 74 (1994) 2944-2948.
 - [27] A. Roy, S. Govil, and R. Miranda, An algorithm to generate Radial Basis Function (RBF)-like nets for classification problems, *Neural Networks* 8 (1995) 179-201.
 - [28] D. B. Fogel, E. C. Wasson, and E. M. Boughton, Evolving neural networks for detecting breast cancer, *Cancer Letters* 96 (1995) 49-53.
 - [29] D. B. Fogel, E. C. Wasson EC, and V. W. Porto, A step toward computer-assisted mammography using evolutionary programming and neural networks, *Cancer Letters* 119 (1997) 93-97.
 - [30] B. Sahiner, H.-P. Chan, N. Petrick, D. Wei, M. A. Helvie, D. D. Adler, and M. M. Goodsitt, Classification of mass and normal breast tissue: A convolution neural network classifier with spatial domain and texture images, *IEEE Transactions on Medical Imaging* 15 (1996) 598-610.
 - [31] R. Setiono, Extracting rules from pruned neural networks for breast cancer diagnosis, *Artificial Intelligence in Medicine* 8 (1996) 37-51.
 - [32] H. B. Burke, P. H. Goodman, D. B. Rosen, D. E. Henson, J. N. Weinstein, F. E. Harrell, J. J. R. Marks, D. P. Winchester, D. G. Bostwick, Artificial Neural Networks improve the accuracy of cancer survival prediction, *Cancer* 79 (1997) 857-862.
 - [33] D. Furundzic, M. Djordjevic, and A. J. Bekic, Neural networks approach to early breast cancer detection, *Syst. Architect.* 44 (1998) 617-633.
 - [34] C. A. Peña-Reyes and M. Sipper, A fuzzy-genetic approach to breast cancer diagnosis, *Artificial Intelligence in Medicine* 17 (1999) 131-155.
 - [35] R. Setiono, Generating concise and accurate classification rules for breast cancer diagnosis, *Artificial Intelligence in Medicine* 18 (2000) 205-219.
 - [36] D. West and V. West Model selection for a medical diagnostic decision support system: a breast cancer detection case, *Artificial Intelligence in Medicine* 20 (2000) 183-204.
 - [37] H. A. Abbass, An evolutionary artificial networks approach to breast cancer, *Artificial Intelligence in Medicine* 25 (2002) 265-281.
 - [38] M. J. Aragones, A. G. Ruiz, R. Jimenez, M. Perez, and E. A. Conejo, A combined neural network and decision

- trees model for prognosis of breast cancer relapse, *Artificial Intelligence in Medicine* 27 (2003) 45-53.
- [39] P. Meesad and G. Yen, Combined numerical and linguistic knowledge representation and its application to medical diagnosis, *IEEE Transactions on Systems, Man, and Cybernetics, Part A: Systems and Humans* 3 (2003) 206-222.
- [40] C. M. Chen, Y. H. Chou, K. C. Han, G. S. Hung, C. M. Tiu, H. J. Chiou, and S. Y. Chiou, Breast lesions on sonograms: Computer aided diagnosis with nearly setting-independent features and Artificial Neural Networks, *Radiology* 226 (2003) 504-514.
- [41] T. Kiyani and T. Yildirim, Breast cancer diagnosis using statistical neural networks, *Journal of Electrical and Electronics Engineering* 14 (2004) 1149-1153.
- [42] S. M. Chou, T. S. Lee, Y. E. Shao, and I. F. Chen, Mining the breast cancer pattern using Artificial Neural Networks and multivariate adaptive regression splines, *Expert Syst. Applications* 27 (2004) 133-142.
- [43] A GAs based approach for mining breast cancer pattern, T.-C. Chen and T.-C. Hsu, *Expert Syst. Applications* 30 (2006) 674-681.
- [44] J. Nahar, Y. P. P. Chen, and S. Ali, Kernel based Naive Bayes Classifier for breast cancer prediction, *Journal of Biological Systems*, 15 (2007) 1725.
- [45] D. A. Elizondo, R. Birkenhead, M. Góngora, E. Tailard, P. Luyima, Analysis and test of efficient methods for building recursive deterministic perceptron neural networks, *Neural Networks* 20 (2007) 1095-1108.
- [46] E. D. Übeyli, Implementing automated diagnostic systems for breast cancer predictions, *Expert Syst. Applications* 33 (2007) 1054-1062.
- [47] L. Jelen, T. Fevens, and A. Krzyzak, Classification of breast cancer malignancy using cytological images of Fine Needle Aspiration Biopsies, *International Journal of Applied Mathematics and Computer Science* 18 (2008) 75-83.
- [48] C. L. Huang, H.-C. Liao, and M.-C. Chen, M.-C. (2008). Prediction, model building and feature selection with support vector machines in breast cancer diagnosis, *Expert Syst. Applications* 34 (2008) 5785-5787.
- [49] M. F. Akay, SVMs combined with feature selection for breast cancer diagnosis, *Expert Syst. Applications* 36 (2009) 3240-3247.
- [50] T. S. Subashini, V. Ramalingam, and S. Palanivel, Breast mass classification based on cytological patterns using RBFNN and SVM, *Expert Syst. Applications* 36 (2009) 5284-5290.
- [51] M. Karabatak and M. C. Ince, An expert system for detection of breast cancer based on association rules and neural network, *Expert Syst. Applications* 36 (2009) 3465.
- [52] L. Liang, F. Cai, and Vladimir Cherkassky, Predictive learning with structured (grouped) data, *Neural Networks* 22 (2009) 766-773.
- [53] F. Paulin and A. Santhakumaran, Extracting rules from feed forward neural networks for diagnosing breast cancer, *CiiT International Journal of Artificial Intelligent Systems and Machine Learning* 1 (2009) 143-146.
- [54] F. Paulin and A. Santhakumaran, Back propagation neural network by comparing hidden neurons: Case study on breast cancer diagnosis, *International Journal of Computer Applications* (0975 8887) 2 (2010) 40-44.
- [55] F. Paulin and A. Santhakumaran, Classification of breast cancer by comparing back propagation training algorithms, *International Journal on Computer Science and Engineering* 3 (2011) 327-332.
- [56] R. T. Peres and C. E. Pedreira, A new localglobal approach for classification, *Neural Networks* 23 (2010) 887-891.
- [57] M. Fallahnezhad, M. H. Moradi, and S. Zaferanlouei, A Hybrid Higher Order Neural Classifier for handling classification problems, *Expert Syst. Applications* 38 (2011) 386-393.
- [58] H.-L. Chen, B. Yang, J. Liu, and D.-Y. Liu, A support vector machine classifier with rough set-based feature selection for breast cancer diagnosis, *Expert Syst. Applications* 38 (2011) 9014-9022.
- [59] A. Marcano-Cedeño, J. Quintanilla-Domínguez, and D. Andina WBCD breast cancer database classification applying artificial metaplasticity neural network, *Expert Syst. Applications* 38 (2011) 9573-9579.
- [60] H. A. Abd Elgader and M. H. Hamza, Breast cancer diagnosis using artificial intelligence neural networks, *J. Sc. Tech.* 121 (2011) 159-171.
- [61] M. Kowal, P. Filipczuk, A. Obuchowicz, and J. Korbicz, Computer-aided diagnosis of breast cancer using Gaussian mixture cytological image segmentation, *Journal of Medical Informatics & Technologies* 17 (2011) 257-262.
- [62] M. Blachnik and W. Duch, LVQ algorithm with instance weighting for generation of prototype-based rules, *Neural Networks* 24 (2011) 824-830.
- [63] Y. M. George, B. M. Elbagoury, H. H. Zayed, and M. I. Roushdy, Breast fine needle tumor classification using neural networks, *IJCSI International Journal of Computer Science Issues* 9 (2012) 247-256.
- [64] A. Aloraini, Different machine learning algorithms for breast cancer diagnosis, *International Journal on Artificial Intelligence Applications* 3 (2012) 11-29.
- [65] B. Gu, J.-D. Wang, Y.-C. Yud, G.-S. Zheng, Y.-F. Huang, and T. Xu, Accurate on-line ν -support vector learning, *Neural Networks* 27 (2012) 51-59.
- [66] R. Savitha, S. Suresh, and N. Sundararajan, A meta-cognitive learning algorithm for a Fully Complex-valued Relaxation Network, *Neural Networks* 32 (2012) 209-218.
- [67] E. Alkim, E. Gürbüz, and E. Kilic, A fast and adaptive automated disease diagnosis method with an innovative neural network model, *Neural Networks* 33 (2012) 88-96.
- [68] A. H. Chen, and C. Yang, The improvement of breast cancer prognosis accuracy from integrated gene expression and clinical data, *Expert Syst. Applications* 39 (2012) 4785-4795.
- [69] J. Nahar, I. Tasadduq, K. S. Tickle, A. B. M. Shawkat Ali, Y.-P. P. Chen, Computational intelligence for microarray data and biomedical image analysis for the early diagnosis of breast cancer, *Expert Syst. Applic.* 39 (2012) 12371-12377.
- [70] C. P. Utomo, A. Kardiana, and R. Yuliwulandari, Breast Cancer diagnosis using Artificial Neural Networks with Extreme Learning Techniques, *International Journal of Advanced Research in Artificial Intelligence* 3 (2014) 10-14.
- [71] B. Zheng, S. W. Yoon, and S. S. Lam, Breast cancer diagnosis based on feature extraction using a hybrid of K-means and support vector machine algorithms, Ex-

- pert Sys. Applications 41 (2014) 1476-1482.
- [72] J. Dheeba, N. A. Singh, and S. T. Selvi, Computer-aided detection of breast cancer on mammograms: A swarm intelligence optimized wavelet neural network approach, *Journal of Biomedical Informatics* 49 (2014) 4552.
- [73] M. Seera and C. P. Lim, A hybrid intelligent system for medical data classification, *Expert. Sys. Applications* 41 (2014) 2239-2249.
- [74] A. Bhardwaj and A. Tiwari, Breast cancer diagnosis using genetically optimized neural network model, *Expert Syst. Applications* 42 (2015) 4611-4620.
- [75] A. Mert, N. Z. Kilic, E. Bilgili, and A. Akan, Breast cancer detection with reduced feature set, *Computational and Mathematical Methods in Medicine* (2015) 1-11.
- [76] K. B. Nahato, H. K. Nehemiah, and A. Kannan, Knowledge mining from clinical datasets using rough sets and backpropagation neural network, *Computational Mathematical Methods in Medicine* (2015) 113.
- [77] M. Karabatak, A new classifier for breast cancer detection based on Naive Bayesian, *Measurement* 72 (2015) 32-36.
- [78] S. Kim, Z. Yu, R. M. Kil, and M. Lee, Deep learning of support vector machines with class probability output networks, *Neural Networks* 64 (2015) 19-28 (2015).
- [79] A. M. Abdel-Zaher and A. M. Eldeib, Breast cancer classification using deep belief networks, *Expert Syst. Applications* 46 (2016) 139-144.
- [80] E. A. Mohammed, C. T. Naugler, and B. H. Far, Breast tumor classification using a new OWA operator, *Expert Syst. Applications* 61 (2016) 302-313.
- [81] V. Chaurasia, Saurabh Pal, and B. B. Tiwari, Prediction of benign and malignant breast cancer using data mining techniques, *Journal of Algorithms & Computational Technology* 12 (2018) 119-126.
- [82] P. Chao, T. Mazeri, B. Sun, N. B. Weingartner, and Nussinov, The stochastic replica approach to machine learning: Stability and parameter optimization [arXiv:1708.05715].
- [83] R. M. Rangayyan, F. J. Aires, and J. E. L. Desautels, A review of computer-aided diagnosis of breast cancer: Toward the detection of subtle signs, *J. Franklin Inst.* 344 (2007) 312-348.
- [84] P. Sadjja, Machine Learning for Detection and Diagnosis of Diseases, *Annual Review of Biomedical Engineering* 8 (2006) 537-565.
- [85] J. A. Cruz and D. S. Wishart, Applications of machine learning in cancer prediction and prognosis, *Cancer Informatics* 2 (2006) 59-77.
- [86] H. You and G. Rumba, Comparative study of classification techniques on breast cancer FNA biopsy data, *International Journal of Artificial Intelligence and Interactive Multimedia* 1 (2010) 6-13.
- [87] M. M. Beg and M. Jain, An analysis of the methods employed for breast cancer diagnosis, *International Journal of Research in Computer Science* 2 (2012) 25-29.
- [88] H. Asri, H. Mousannif, H. Al Moatassime, and T. Noel, Use of machine learning algorithms for breast cancer risk prediction and diagnosis, *Procedia Computer Science* 83 (2016) 1064-1069.
- [89] D. Bazazeh and R. Shubair, Comparative study of machine learning algorithms for breast cancer detection and diagnosis, in *Fifth International Conference on Electronic Devices, Systems and Applications*, Ras Al Khaimah, United Arab Emirates (IEEE, New York, 2016), DOI: 10.1109/ICEDSA.2016.7818560.
- [90] S. K. Mandal, Performance analysis of data mining algorithms for breast cancer cell detection using Naive Bayes, logistic regression, and decision tree, *International Journal of Engineering and Computer Science* 6 (2017) 20388-20391.
- [91] W. Yue, Z. Wang, H. Chen, A. Payne, and X. Liu, Machine learning with applications in breast cancer diagnosis and prognosis, *Designs* 2, 13, (2018) 1-17.
- [92] I. Kononenko, Machine learning for medical diagnosis: History, state of the art & perspective, *Artificial Intelligence in Medicine* 23 (2001) 89-109.
- [93] W. Schwarzer, W. Vach, and M. Schumacher, On the misuses of artificial neural networks for prognostic and diagnostic classification in oncology, *Statistics in Medicine* 19 (2005) 541-561.
- [94] S.-H. Liao, Expert system methodologies and applications – a decade review from 1995 to 2004, *Expert Syst. Applications* 28 (2005) 93-103.
- [95] P. J. Lisboa and A. F.G. Taktak, The use of artificial neural networks in decision support in cancer: A systematic review, *Neural Networks* 19 (2006) 408-415.
- [96] R. O. Duda and P. E. Hart, *Pattern Classification and Scene Analysis* (Wiley & Sons, New York, 1973).
- [97] C. M. Bishop, *Neural Networks for Pattern Recognition* (Clarendon Press, Oxford, 1996).
- [98] R. Neal, *Bayesian Learning of Neural Networks* (Springer, New York, 1996).
- [99] V. Vapnik, *Statistical Learning Theory* (Wiley, New York, 1998).
- [100] S. Haykin, *Neural Networks: A Comprehensive Foundation* (Prentice Hall, Upper Saddle River, NJ, 1999).
- [101] T. Elomaa, H. Mannila, and H. Toivonen (Eds.), *Machine Learning 2002*, 13th European Conference on Machine Learning, Helsinki, Finland, August 2002 Proceedings, Springer Lecture Notes in Artificial Intelligence (Springer, Berlin, 2002).
- [102] J. W. Clark, K. A. Gernoth, S. Dittmar, and M. L. Ristig, Higher-Order probabilistic perceptrons as Bayesian inference engine, *Phys. Rev. E* 59 (1999) 661-674.
- [103] F. Rosenblatt, *Principles of Neurodynamics* (Spartan Books, Washington D. C., 1962).
- [104] J. W. Clark, M. L. Ristig, and Lindenau, *Scientific Applications of Neural Nets*, Springer Lecture Notes in Physics, Vol. 522 (Springer-Verlag, Berlin, 1999).
- [105] B. B. Mandelbrot, *The Fractal Geometry of Nature* (W. H. Freeman, New York, 1997).
- [106] M. L. Minsky and S. A. Papert, *Perceptrons*, Expanded Edition (MIT Press, Cambridge, MA, 1987).
- [107] D. W. Ruck, S. K. Rogers, M. Kabrisky, M. E. Oxley, and B. W. Suter, The multilayer perceptron as an approximation to a Bayes optimal discriminant function, *IEEE Trans. Neural Netw.* 1 (1990) 296-298.
- [108] E. A. Wan, Neural network classification: a Bayesian interpretation, *IEEE Trans. Neural Netw.* 1 (1990) 303-305.
- [109] M. D. Richard and R. P. Lippmann, Neural network classifiers estimate Bayesian *a posteriori* probabilities, *Neural Comput.* 3 (1991) 461-483.
- [110] S. Kullback, *Information Theory and Statistics* (Wiley, New York, NY, 1959).